



Modified Dickson Charge Pump and Control Algorithms for a Solar Powered Induction Motor with Open End Windings

Riya Anna Thomas^(✉) and N. Reema

Electrical and Electronics, Sree Buddha College of Engineering, Pattoor, India
312riya94@gmail.com, n.reema3@gmail.com

Abstract. Induction motors are the widely used machines in many industrial applications. But the induction motors results in high starting current, occurrence of common mode voltages, difficult to control etc. This work proposes controlling of a dual inverter fed induction motor with open end stator windings. This system is functioned using an integrated control which includes Perturb and Observe maximum power point tracking algorithm and space vector pulse width modulation technique. A boosting converter with a high voltage gain is also proposed which requires no chemical storage elements such as batteries and make the system more effective. Space vector modulation is designed such that it excludes the common mode voltages generated. The modeling of dual inverter served induction motor with open end windings, PV system, MPPT algorithm, Dickson charge pump and switching of inverters using modulation by space vector has been done and the output waveforms obtained are analyzed.

Keywords: Common mode voltage · Open end winding induction motor
Space vector modulation

1 Introduction

One of the efficient solution for the utilization of resources is the use of systems delivered by photovoltaic solar energy. Among different machines, induction machines are most widely used due to many advantages such as low cost, ease of operation, durability, high starting torque etc. In this paper, a three level dual inverter fed open end winding induction motor (OEWIM) is proposed to overcome the shortcomings of conventional induction motor. Vast works were carried out for different inverter topologies [5–8] and different modulation schemes [9, 10] for OEWIM. In this machine stator windings are open and the supply is given from both sides and inverters are connected at either ends to obtain the multilevel output. Vast works has been carried out about the different modulation schemes used for open end winding induction motor [11, 12]. This work proposes a zero sequence elimination pulse width modulation scheme for the machine. The system is supplied by solar panel and MPPT algorithm is also used to path the maximum power and space vector modulation scheme is also used for switching of inverters efficiency etc. But the induction motors has certain disadvantages such as difficult to control, occurrence of common mode voltages, high

starting current etc. Several multilevel converter topologies have also remained analysed and suggested during several periods [1–3]. To improve the overall performance neutral point clamped inverters was used which is beneficial over two level H bridge inverter [4]. The multilevel inverter is a feasible.

2 Control Algorithms of OEWIM

The proposed system includes control algorithms for an open end winding induction motor (OEWIM) besides modified Dickson charge pump. OEWIM is simply an induction motor with both the ends of the stator windings are opened. The Fig. 1 shows the block illustration of the proposed system.

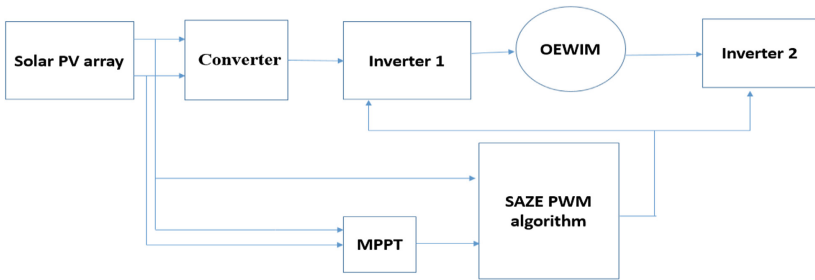


Fig. 1. Block illustration of control algorithms of OEWIM

Nowadays OEWIM received large attention in many applications and has many advantage over conventional induction machine. The proposed system is powered by solar photovoltaic panel and to track the maximum power MPPT algorithm is used. A great voltage gain DC- DC converter is also used to acquire a stable output. The proposed converter is Dickson charge pump voltage multiplier. An OEWIM contains dual inverters on either side of the machine to achieve a 3 level output voltage and supply is provided from both sides of the inverter. The machine can be used for variable speed applications, grid applications, hybrid vehicles etc. Figure 2 illustrates an induction machine with both ends of stator windings are open.

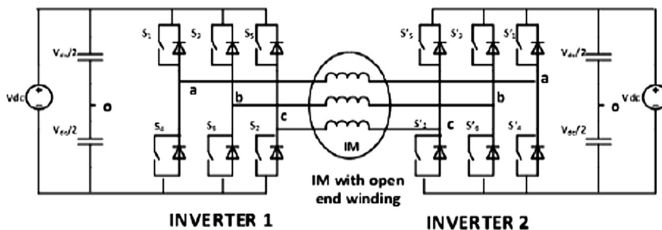


Fig. 2. OEWIM

Since both ends of stator windings are open the switches can be rated at half of the machine power rating and it removes the common mode voltage generated due to switching.

3 Simulation and Results

3.1 Modeling of Induction Motor

Modelling of OEWM is similar to conventional induction motor. For simulating the proposed system, a 4 kW induction motor is modelled with the parameters specified in Table 1.

Table 1. Motor parameters

Parameter	Value	Parameter	Value
Input voltage	400 V	Stator resistance, R_s	1.405 Ω
Stator current	7.2 A	Stator inductance, L_s	0.0058 H
Rated speed	1430 rpm	Moment of inertia, J	0.0131 kg-m ²

The stator and rotor voltage equations are showed below.

$$V_{qs} = R_s i_{qs} + \frac{d\phi_{qs}}{dt} + \omega_e \phi_{ds} \quad (1)$$

$$V_{ds} = R_s i_{ds} + \frac{d\phi_{ds}}{dt} + \omega_e \phi_{qs} \quad (2)$$

$$V_{qr} = R_s i_{qr} + \frac{d\phi_{qr}}{dt} + \omega_e \phi_{dr} \quad (3)$$

$$V_{dr} = R_s i_{dr} + \frac{d\phi_{dr}}{dt} + \omega_e \phi_{qr} \quad (4)$$

The equation for determining torque and rotor speed of induction motor is given by

$$T_e = \frac{3}{2} * \frac{p}{2} * \frac{1}{w_b} (F_{ds} i_{qs} - F_{qs} i_{ds}) \quad (5)$$

$$T_e = T_l + \frac{2}{p} * J * \frac{dw_r}{dt} \quad (6)$$

Figure 3 shows the modeling of induction motor according to the above voltage and torque equations. The results obtained are as follows. Figure 4 shows the input voltage given to the induction motor with an amplitude of 325 V.

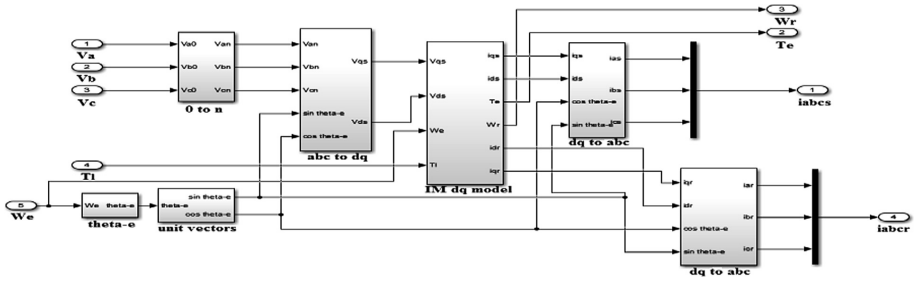


Fig. 3. Modeling of induction motor

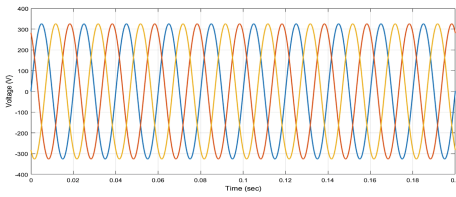


Fig. 4. Input voltage of induction motor

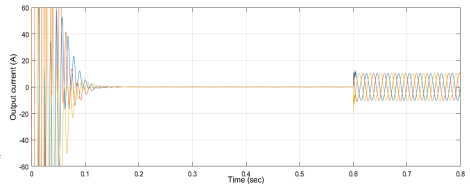


Fig. 5. Output current of induction motor

Figure 5 shows the waveforms of output current, of an induction machine. A step time of 0.6 s is given to the machine, as a result up to 0.6 s the graphs shows the no load reading and after 0.6 s loaded condition is depicted here. The topmost value of the current of about 10.2 A obtained (Figs. 6 and 7).

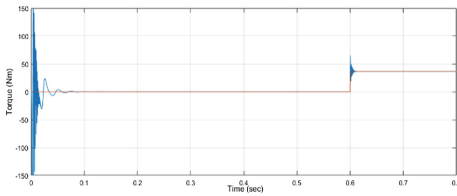


Fig. 6. Torque Vs Time graph

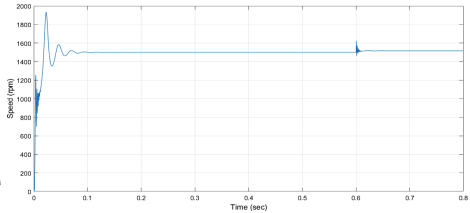


Fig. 7. Speed Vs Time graph

3.2 Modeling of PV System

Solar photovoltaic system is used to supply the machine and is modeled for running a 4 kW OEWM. It is modeled according to the voltage current characteristic equation.

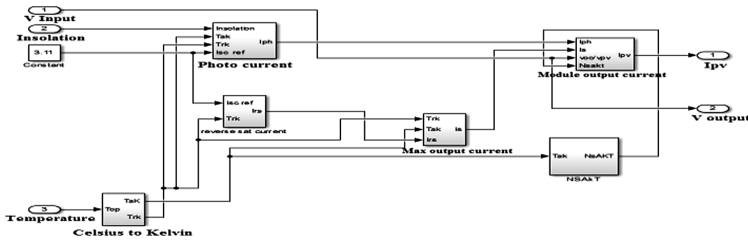


Fig. 8. Modeling of PV system

Figure 8 shows the modeling of photovoltaic system in MATLAB according to the voltage current characteristics equation given below:

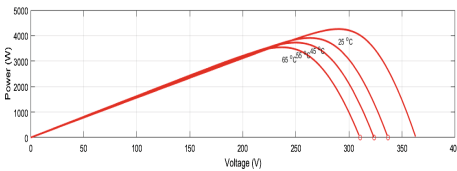


Fig. 9. PV characteristics

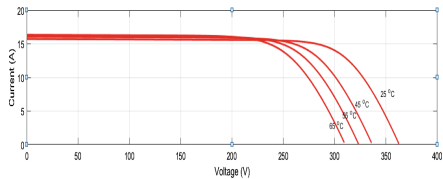


Fig. 10. VI characteristics

$$I = I_{ph} - I_s \left[\exp\left(\frac{q(V + IR_s)}{kT_c A}\right) - 1 \right] - \frac{V + IR_s}{R_{sh}} \tag{7}$$

Figures 9 and 10 shows the PV and VI characteristics obtained during varying temperatures such as 25 °C, 35 °C, 45 °C etc. To obtain the required output power, in 3 rows about 23 panels should be connected in series.

3.3 Modeling of MPPT Algorithm

MPPT algorithm can track maximum power and P&O method, one of the most simplest method is proposed here. Figure 11 shows the modeling of MPPT algorithm and the output obtained is used to trigger the converter switches.

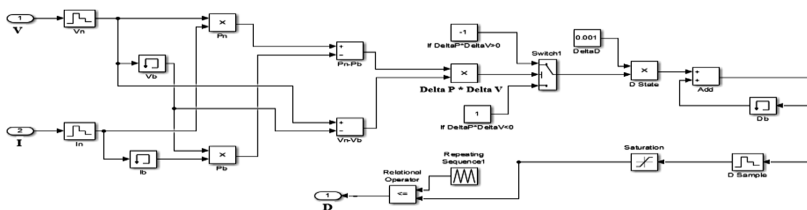


Fig. 11. Modeling of MPPT algorithm

3.4 Modeling of Converter

To obtain a stable output a converter is also proposed in this circuit. A Dickson charge pump voltage multiplier is used which had a high voltage gain and removes the need of chemical storages such as batteries (Table 2).

Table 2. Converter parameters

Parameter	Value	Parameter	Value
Input voltage	20 V	L_1	100 μ H
Output voltage	400 A	L_2	100 μ H
Load resistance	800 Ω	VM capacitors	60 μ F

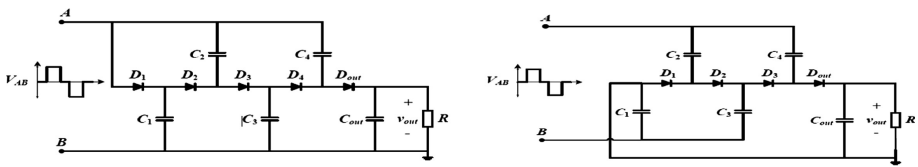


Fig. 12. Dickson charge pump voltage multiplier

Figure 12 shows the circuit of conventional and modified Dickson charge pump and Fig. 13 shows the different modes of operation of Dickson charge pump.

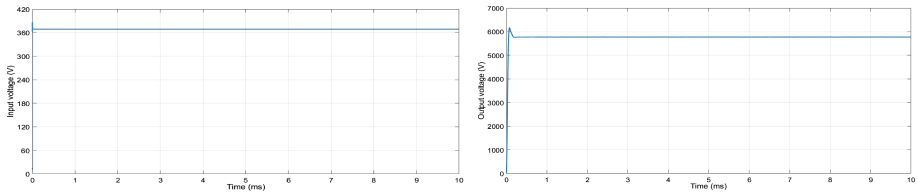


Fig. 13. Input and output of dickson charge pump voltage multiplier at 1000 W/m² and 25 °C

The circuit works by the charging and discharging of the capacitors in the circuit. It has three modes of operation, either two switches will be ON or either of the switches will be ON. The graph shows the input and output voltage at 1000 W/m² and 25 °C is shown in Fig. 13.

3.5 Modeling of OEWM and Space Vector Modulation

Modeling of OEWM is given by subtracting the difference of pole numbers of both the inverters which can be seen in Fig. 14. The equations below are used for converting abc to dq coordinate

$$V_d = \frac{2}{3} \left(V_a \sin \omega t + V_b \sin \left(\omega t - \frac{2\pi}{3} \right) + V_c \sin \left(\omega t + \frac{2\pi}{3} \right) \right) \quad (8)$$

$$V_q = \frac{2}{3} \left(V_a \cos \omega t + V_b \cos \left(\omega t - \frac{2\pi}{3} \right) + V_c \cos \left(\omega t + \frac{2\pi}{3} \right) \right) \quad (9)$$

$$V_0 = \frac{1}{3} (V_a + V_b + V_c) \quad (10)$$

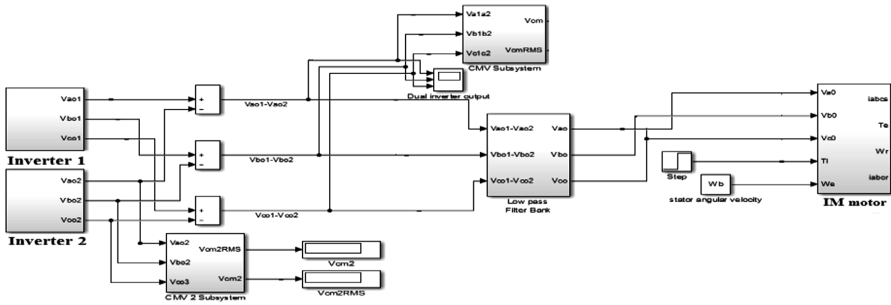


Fig. 14. Modeling of OEWM

The below equations shows the determination of time duration

$$T_a = \frac{\sqrt{3} * T_Z * V_{ref}}{V_{dc}} \left(\sin \frac{n}{3} \pi \cos \alpha - \cos \frac{n}{3} \pi \sin \alpha \right) \quad (11)$$

$$T_b = \frac{\sqrt{3} * T_Z * V_{ref}}{V_{dc}} \left(-\sin \frac{n-1}{3} \pi \cos \alpha + \cos \frac{n-1}{3} \pi \sin \alpha \right) \quad (12)$$

Figure 15 shows the space vector modulation of the dual inverter. The inverters are pulsed by space vector modulation scheme and is modeled rendering to the above equations.

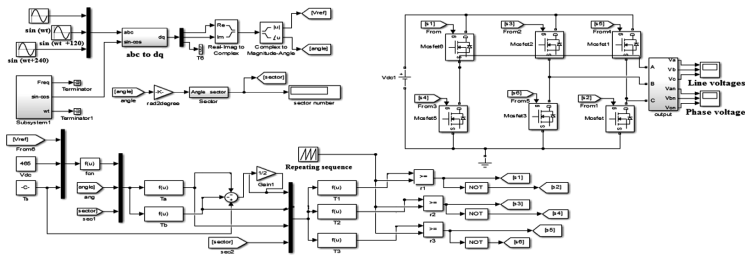


Fig. 15. Modeling inverter and space vector modulation scheme

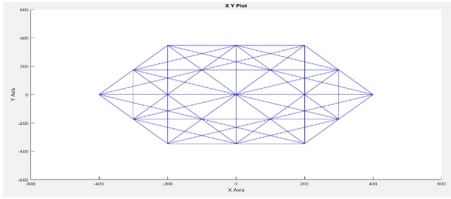


Fig. 16. Space vector of dual inverters

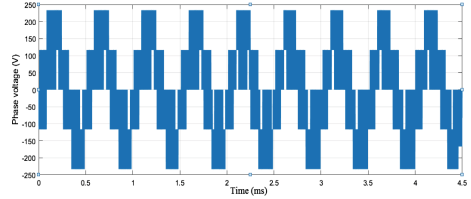


Fig. 17. Dual inverter voltage

The modulation scheme has a total of space vector locations of about 64 which can be depicted from the Fig. 16. Figure 17 shows the dual inverter output voltage obtained by space vector modulation.

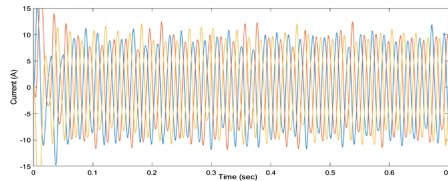


Fig. 18. Output current of OEWM

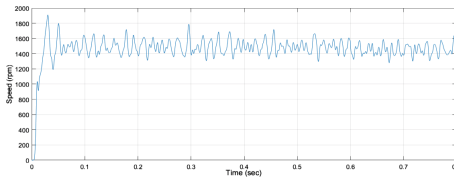


Fig. 19. Speed characteristics

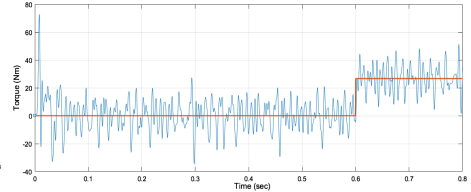


Fig. 20. Torque characteristics

Figures 18, 19 and 20 shows the output current, speed and torque of an OEWM. The dual inverter is modeled and the difference in voltages of inverters is given to induction motor to obtain the modeling of OEWM. A 0.6 s a step load is applied and the variation during load can be shown in the figure. The use of OEWM over conventional machine excludes the common mode voltages generated.

4 Conclusion

Induction machine with stator end windings open are analysed with dual inverters connected to the open end winding induction machine. This machine offers many advantages over conventional induction machine and can be used for many applications such as variable speed, grid, pumping applications etc. Modeling of OEWM with three level inverter, PV system, MPPT are modeled and different output waveforms are analyzed.

References

1. Wheeler, P., Xu, L., Meng, Y., Empringham, L., Klumpner, C., Clare, J.: Analysis of multilevel matrix converter topologies. In: Proceedings of 4th IET Conference Power Electronics, pp. 286–293 (2008)
2. Rodriguez, J., JihSheng, L., Zheng, P.: Multilevel inverters, a survey of topologies, controls. IEEE Trans. Ind. Electron. **49**(4), 719–724 (2003)
3. Bernet, S., Steimer, P.K., Rodriguez, J., Lizama, I.E.: A review on neutral point clamped inverters. IEEE Trans. Ind. Electron. **58**(9), 229–2220 (2011)
4. Jiao, Y., Lu, S., Lee, F.C.: Switching performance optimization of a high power high frequency 3 level active neutral point clamped leg. IEEE Trans. Power Electron. **29**(7), 3245–3266 (2014)
5. Rajeevan, P., Sivakumar, K., Gopakumar, K., Patel, C., Abu, H.: A 9 level inverter topology for medium voltage induction motor drive with oewim. IEEE Trans. Ind. Electron. **60**(9), 3627–3636 (2013)
6. Somasekar, V., Vennugopal Reddy, B., Sivakumar, K.: A 4 level inversion scheme for a 6-*n*-pole OEWM drive for a better-quality DC link utilization. IEEE Trans. Ind. Electron. **57**(9), 4656–4672 (2014)
7. Kaarthik, R.S., Gopakumar, K., Mathew, J., Undeland, T.: Medium voltage drive for IM with multilevel dodecagonal voltage space vectors with symmetric triangles. IEEE Trans. Ind. Electron. **63**(1), 75–87 (2014)
8. Kouro, S., Rodriguez, J., Bin, W., Bernet, S., Perez, M.: Powering the future of industry, Highpower malleable speed drive topologies. IEEE Ind. Appl. Mag. **15**(4), 26–39 (2012)
9. Betin, F.: Developments in electrical machines control: Samples for standard, fault-tolerant, sensorless, techniques. IEEE Ind. Electron. Mag. **8**(2), 43–55 (2014)
10. Meinguet, F., Sandulescu, P., Kestelyn, X., Semail, E.: Fault-tolerant operation of an OEW 5phase PMSM drive with inverter faults. In: Proceedings Conference IEEE Industrial Electronics, pp. 5191–5196 (2013)
11. Venugopal Reddy, B., Somasekhar, V.T., Kalyan, Y.: Decoupled space-vector PWM strategies for a four-level asymmetrical open-end winding induction motor drive with waveform symmetries. IEEE Trans. Ind. Electron. **58**(11), 5130–5141 (2011)
12. Jacob, B., Baiju, M.R.: Vector-quantized space-vector-based spread spectrum modulation scheme for multilevel inverters using the principle of oversampling ADC. IEEE Trans. Ind. Electron. **60**(8), 2969–2977 (2013)